CALCULATION OF EDDY CURRENT FIELDS FOR COILS OF ARBITRARY SHAPE

R.E. Beissner

Southwest Research Institute
6220 Culebra Road
San Antonio, TX 78228-0510

J.A.G. Temple

Theoretical Physics Division
Harwell Laboratory
Oxon OX11 0RA, U.K.

INTRODUCTION

In the design of an eddy current inspection device, it is useful to have available a means of visualizing the eddy current distribution produced in the material to be tested. This is evidenced by the widespread use of the early models of Dodd and Deeds [1], who provided analytic solutions for the field in a number of axisymmetric probe geometries. The analytic approach was later extended [2-4] to include a more general class of coils, and was applied to the case of a circular, air-core horizontal coil [4].

While the generalized analytic approach can, in principle, be applied to coils of any shape, extending calculations beyond the treatment of circular coils has a practical difficulty. This results from the formulation, which, in general, requires a numerical integration over the coil volume. In this paper, a simple approach is presented for performing the necessary integral and computing the eddy current field for coils of arbitrary shape and orientation.

The treatment is based on the use of the magnetic scalar potential to describe the field produced by the coil in free space. The first section of the paper shows how the general analytic solution for the field in a half-space can be recast in terms of the normal derivative of this potential, thus reducing the problem to the calculation of the scalar potential. Use is then made of the equivalence of the scalar potential at a point in space and the solid angle subtended by the coil at that point [5] to provide a new algorithm for calculation of the potential. The final expression for the eddy current field is a convolution integral involving the normal derivative of the free-space scalar potential and a known, analytic kernel. After completion of the theoretical discussion in the first section, the remainder of the paper focuses on applications to rectangular, triangular, and split-D coils, with examples of the effects of coil orientation on the eddy current field. A preliminary account of the theory described here has been published elsewhere [6].

Review of Progress in Quantitative Nondestructive Evaluation, Vol. 9
Edited by D.O. Thompson and D.E. Chimenti
Plenum Press, New York, 1990

THEORY

The geometry of the calculation is as follows: the conductor surface is the xy plane, and the coil is in air at $z > 0$. The desire is to calculate the eddy current distribution in planes parallel to the xy plane at negative values of z; i.e., on plane surfaces within the conductor.

The basic theory describing the field within the conductor is presented in Ref. 3. In that work, it is shown that the components of the current density can be written as derivatives of a Hertz potential. This, in turn, is written as a two-dimensional Fourier integral containing the two-dimensional transform of the magnetic field produced by the coil in free space. The incident field on the xy plane can be written quite generally as the transform of the normal derivative of a scalar potential, which is, again, the potential in free space. Thus, if $\vec{j}$ is the current density, Ψ is the Hertz potential, and B_z^0 is the normal component of the flux density at z=0, then from Ref. 3,

$$\vec{j}(\vec{\rho},z) = \hat{x}\frac{d\Psi}{dy} - \hat{y}\frac{d\Psi}{dx} \tag{1}$$

and

$$\Psi(\vec{\rho},z) = \frac{i\omega}{\pi}\int \tilde{B}_z^0(\vec{k},0)\frac{e^{i\vec{k}\cdot\vec{\rho}+\lambda z}}{k(\lambda+k)}d^2k, \tag{2}$$

with

$$\lambda = \sqrt{k^2 - \frac{2i}{\delta^2}} \tag{3}$$

and

$$\tilde{B}_z^0(\vec{k},0) = -\frac{\mu_0}{2\pi}\int\left(\frac{d\Phi_0}{dz}\right)_{z=0} e^{-i\vec{k}\cdot\vec{\rho}'}d^2\rho'. \tag{4}$$

Substitution in the expression for the current density, followed by a change in the order of integration, leads to the following integral expression involving the normal derivative of the potential and a kernel which can be evaluated analytically in terms of Kelvin functions:

$$\vec{j}(\vec{\rho},z) = -\frac{1}{\pi}\int\left(\frac{d\Phi_0}{dz}\right)_{z=0}\frac{\hat{y}(x-x') - \hat{x}(y-y')}{|\vec{\rho}-\vec{\rho}'|}R(|\vec{\rho}-\vec{\rho}'|,z)d^2\rho' \tag{5}$$

where

$$R(r,z) = \int_0^\infty e^{\lambda z}J_1(kr)k(k-\lambda)dk. \tag{6}$$

This equation is the final form of the relation between the incident field and the current density at a point specified by the vector $\vec{\rho}$, which lies in the xy plane, and the depth z below the surface.

To make use of this model, an efficient way is needed to calculate the normal derivative of the free space potential on the z=0 plane below the exciter coil. This is the next part of the development.

Use is made of the proportionality of the scalar potential at a point in space and the solid angle subtended by a current loop at that point. The potential for a winding of finite height and thickness is then obtained by integrating the potential for a winding of infinitesimal height and thickness over the actual dimensions of the coil. Derivatives of the potential are obtained from the differences in the potential at closely spaced points.

The central problem, then, is the calculation of the potential produced by, or equivalently the solid angle subtended by, a current loop of arbitrary shape at a point in space. This is done by approximating the area of the loop by a series of planar triangles, as indicated in Figure 1, so that the solid angle of the loop is then the sum of solid angles of the triangles. The solid angle of a triangle is, by definition, the area of the spherical triangle obtained by projecting the triangle onto the unit sphere about the point in question. The potential at that point is then proportional to the sum of areas of spherical triangles, which can be calculated from elementary spherical trigonometry. This development, along with the current density integral presented earlier, are all that was needed to write a computer code for generating eddy current maps for coils of arbitrary shape.

APPLICATIONS

Because our algorithm is based on a triangular discretization of the coil, the simplest case to treat is a triangular coil like the one shown in Figure 2a. Figure 2b is a map of the eddy current field induced by this coil at a distance of about 1/4 skin depth below the surface.

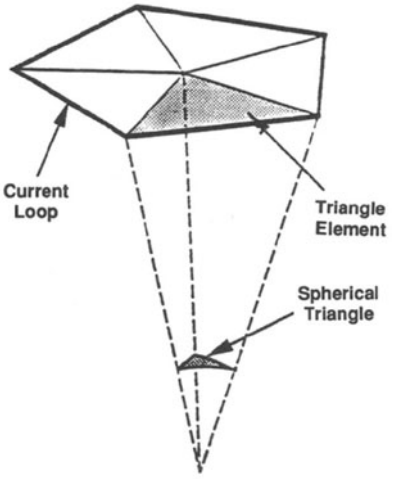

Fig. 1. Calculation of the magnetic scalar potential for an elementary current loop. The potential is proportional to the solid angle subtended by the loop, which, in turn, is equal to the sum of the areas of spherical triangles projected on a unit sphere about the field point.

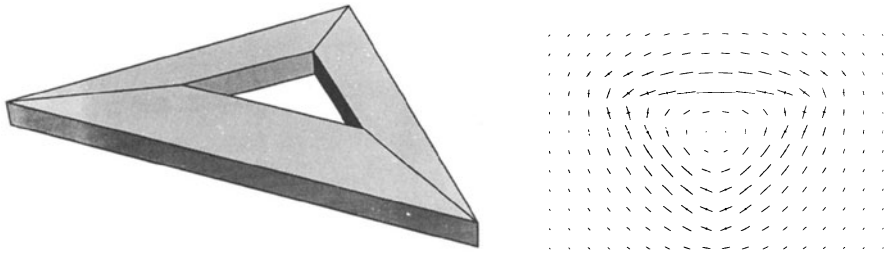

(a) (b)

Fig. 2. A triangular coil (a) and the eddy current distribution (b) produced by the coil. In (b), lines denote the direction and magnitude of the current density; crosses that appear near the vertices of the triangle denote the major and minor axes of the polarization ellipse, as explained in the text and illustrated in Figure 4.

The lines in this figure represent the direction and magnitude of the eddy current field; the triangular pattern of the image current with some rounding of the corners is easily seen. Notice, however, that the field near the vertices of the triangle is represented by crosses instead of lines, which requires some explanation.

To understand the crosses, consider the general expressions for the real, time-dependent components of the eddy current vector at a point in the material,

$$J_x = |j_x| cos(\phi_x - \omega t) \tag{7}$$

and

$$J_y = |j_y| cos(\phi_y - \omega t). \tag{8}$$

The components are characterized by two amplitudes, which generally are different, and by two phase angles, which may also be different for the two components. If these general expressions are squared, the cosine factors are expanded, and the time-dependent factors are eliminated, an equation is obtained that relates J_y to J_x. It turns out that this general equation is the equation of an ellipse [7]. This means that generally the eddy current vector at a point traces out an elliptical figure once per cycle, rather than oscillating back and forth along a straight line.

Figure 3 is an illustration of elliptical polarization. During the course of one cycle, the current vector changes in both direction and magnitude in such a way that its end point traces out an elliptical pattern. To represent this situation graphically in plots of the eddy current field, the major and minor axes of the polarization ellipse have been drawn at each point in the map of the field. This is the meaning of the crosses in the field maps.

At points near the vertices of the triangular coil, where the current tends to make an abrupt change in direction, the field becomes elliptically polarized, as indicated here by the lengths of the major and minor axes. At points well away from the vertices, the length of the minor axes is negligible; and the field is approximately linearly polarized.

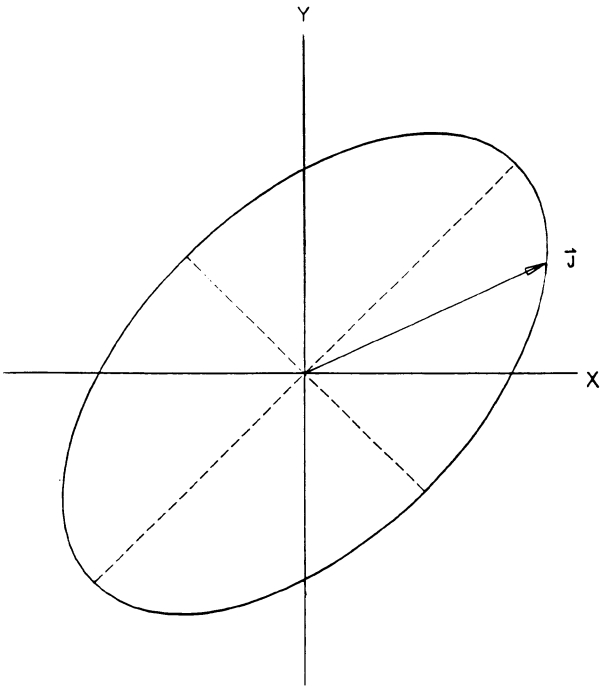

Fig. 3. Illustration of elliptically polarized current density. In the course of one cycle, the end point of the current density vector traces out an ellipse.

Now consider at another simple configuration, a rectangular coil with its plane parallel to the conductor surface, as shown in Figure 4. The field plot in this case is just what one would expect, with some slight evidence of elliptical polarization at the corners and with the current highly concentrated under the coil. But if the coil is turned sideways to the tangential position, as in Figure 5a, the field plot (Figure 5b) shows a more diffuse current distribution and strong elliptical, almost circular polarization near the ends of the coil.

As the final example, the effects of coil tilt, in this case for a split-D coil, were considered. Figure 6a shows two D-shaped windings (seen from above) in the normal configuration with the coil faces parallel to the surface. The current density pattern shown in Figure 6b reflects the split-D configuration with the current flowing clockwise under one winding and counterclockwise under the other.

If the coil is tilted 5 degrees about the axis of symmetry so that one of the D windings is closer to the surface than the other, then the pattern looks like that displayed in Figure 7a. A stronger and more concentrated current is shown on the side where the winding is nearer the surface, and a weaker, more diffuse pattern appears on the other side. Figure 7b shows the effect of tilting the coil in the other direction so that the bottom of the coil is closer to the surface than the top. Again, the result is in agreement with what one would expect based on a qualitative understanding of the behavior of eddy currents.

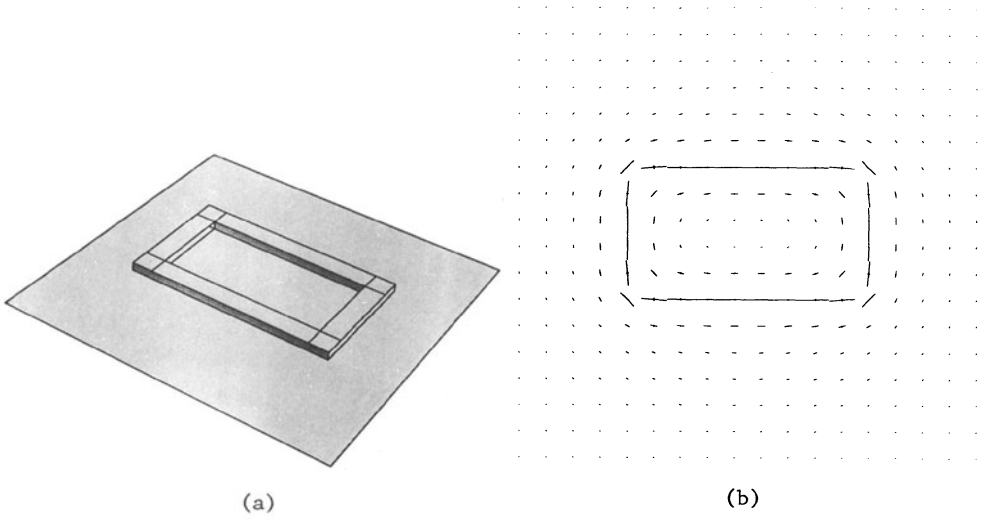

(a) (b)

Fig. 4. Rectangular coil (a) and the corresponding eddy current pattern (b). When the plane of the coil is parallel to the surface of the conductor, the current density is highly concentrated under the coil winding.

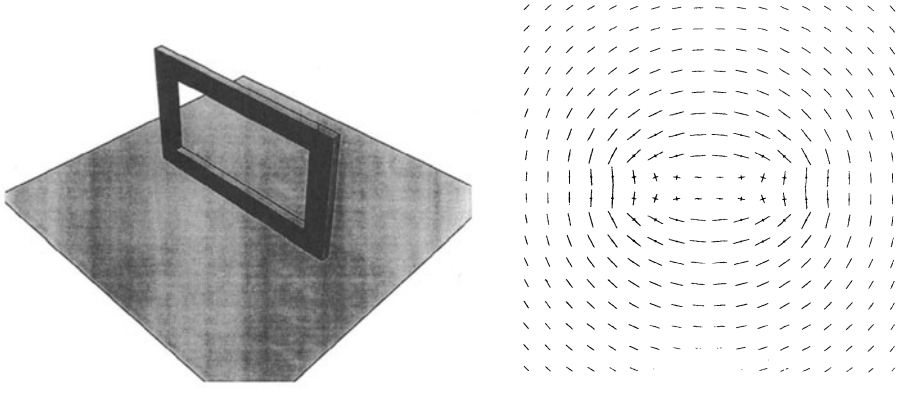

(a) (b)

Fig. 5. Effects of coil orientation. The coil is the same as that shown in Figure 4a, but the plane of the coil is now perpendicular to the surface. The eddy current pattern in (b) is now more diffuse than in Figure 4b, and shows more evidence of elliptical polarization.

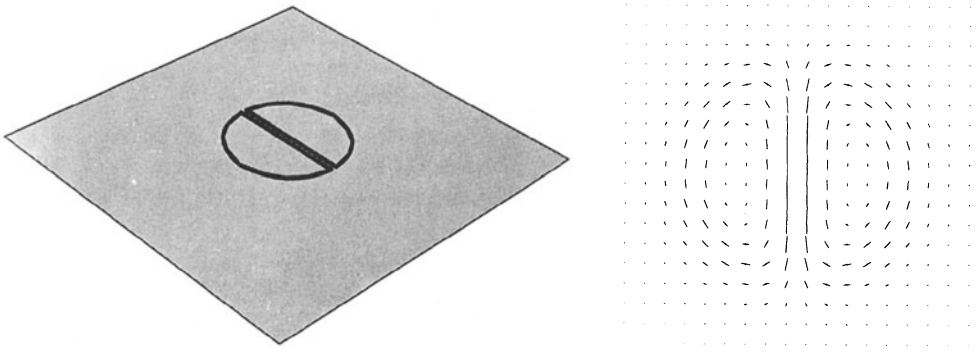

(a) (b)

Fig. 6. Split-D coil configuration (a) and the eddy current field (b) produced when the coils are wound in opposition.

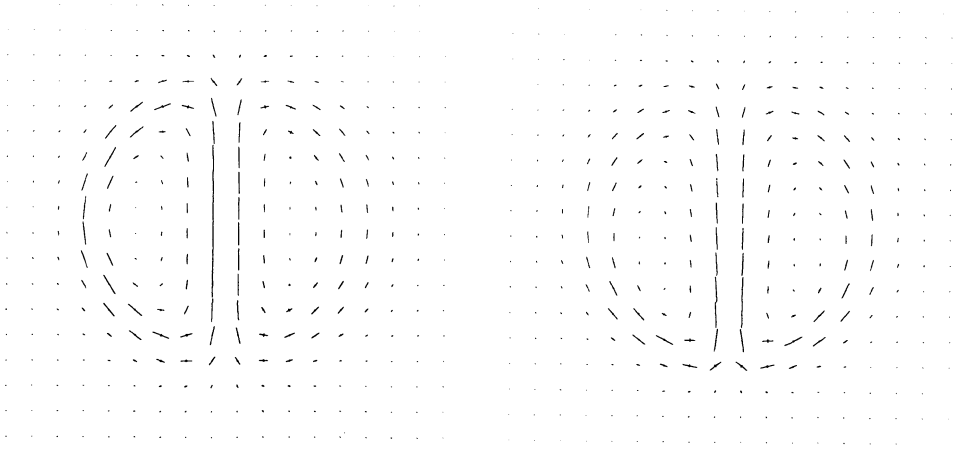

(a) (b)

Fig. 7. Effects of coil tilt on the field of the split-D winding shown in Figure 6. In (a), the coil is tilted so that the left half of the coil is closer to the surface than the right half; in (b), the bottom is closer than the top of the coil.

The whole point to this exercise is, of course, that the algorithm developed during this study enables one to make quantitative predictions of eddy current fields, including the effects of coil geometry and orientation.

SUMMARY

A method was developed for calculating the magnetic scalar potential for a coil of arbitrary shape, which, when combined with a theory of eddy currents under a plane surface, allows one to map the eddy current field produced by the coil. Several examples also demonstrate the applicability of the method to predict the effects of coil geometry and tilt on the eddy current field.

ACKNOWLEDGMENT

This work was sponsored in part by the Center for Advanced Nondestructive Evaluation, operated by the Ames Laboratory, USDOE, for the Air Force Wright Aeronautical Laboratories/Materials Laboratory under Contract No. W-7405-ENG-82 with Iowa State University, and, in part, by the Underlying Programme of the U.K.A.E.A.

REFERENCES

1. C. V. Dodd and W. E. Deeds, J. Appl. Phys. 39, 2829 (1968).
2. J. T. Weaver, Geophys. J. R. Astron. Soc. 22, 83 (1970).
3. R. E. Beissner and M. J. Sablik, J. Appl. Phys. 56, 448 (1984).
4. S. K. Burke, J. Phys. D: Appl. Phys. 19, 1159 (1986).
5. J. A. Stratton, Electromagnetic Theory (McGraw-Hill, New York, 1941), p. 238.
6. R. E. Beissner and J. A. G. Temple, NDT Comm. 4, 142 (1989).
7. J. A. Stratton, Electromagnetic Theory (McGraw-Hill, New York, 1941), p. 279.